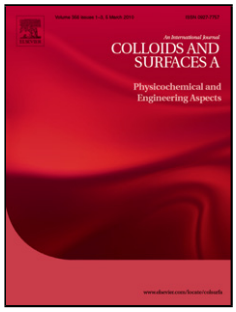

Title: Functionalised novel gemini surfactants as corrosion inhibitors for mild steel in 50 Mm NaCl: experimental and theoretical insights

Authors: Marta Pakiet, Joao Tedim, Iwona Kowalczyk, Bogumił Brycki

PII: S0927-7757(19)30680-6
DOI: https://doi.org/10.1016/j.colsurfa.2019.123699
Article Number: 123699

Reference: COLSUA 123699

To appear in: *Colloids and Surfaces A: Physicochem. Eng. Aspects*

Received date: 3 June 2019
Revised date: 18 July 2019
Accepted date: 19 July 2019

Please cite this article as: Pakiet M, Tedim J, Kowalczyk I, Brycki B, Functionalised novel gemini surfactants as corrosion inhibitors for mild steel in 50 Mm NaCl: experimental and theoretical insights, *Colloids and Surfaces A: Physicochemical and Engineering Aspects* (2019), https://doi.org/10.1016/j.colsurfa.2019.123699

Functionalised novel gemini surfactants as corrosion inhibitors for mild steel in 50 Mm NaCl: experimental and theoretical insights

Marta Pakiet,*[a,b] Joao Tedim[b], Iwona Kowalczyk[a], Bogumił Brycki[a]

[a.] *Laboratory of Microbiocides Chemistry, Faculty of Chemistry, Adam Mickiewicz University in Poznań, Poznań, Poland*

[b.] *Department of Materials and Ceramic Engineering, CICECO – Aveiro Institute of Materials, University of Aveiro, Aveiro, Portugal*

Graphical Abstract

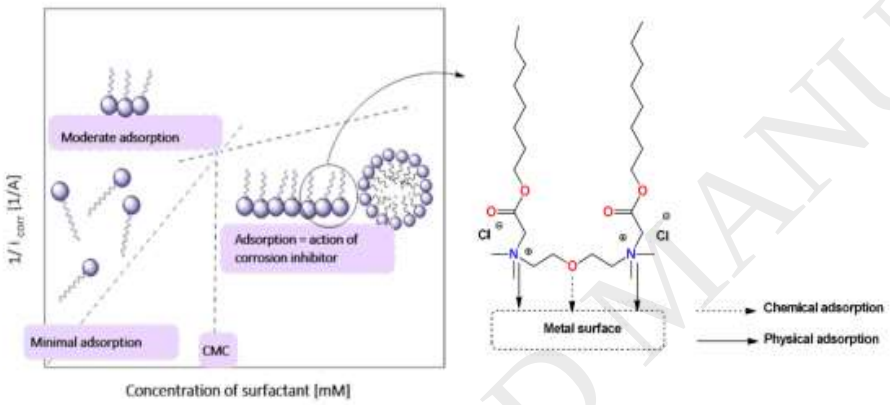

Novel gemini surfactants functionalised with oxygen atom and ester groups were synthesized and characterised by NMR methods. The corrosion inhibiting properties of the synthesized compounds were investigated by potentiodynamic polarization, linear polarization resistance (LPR) and electrochemical impedance spectroscopy (EIS). The results show that inhibition efficiency depends on concentration and the ability to create micelles in aqueous environment, with the highest inhibition efficiency being at around critical micelle concentration (CMC). Furthermore, their inhibition effect was compared against a well-known, commercially available, corrosion inhibitor (benzotriazole) and found to be better for the novel compounds under study in this work. Moreover, the Langmuir adsorption isotherm was found to be suitable for correlating the experimental results with the proposed mechanism of protection. Theoretical studies were based on Density Functional Theory (DFT) and correlation between experimental and theoretical results was determined. These results open perspectives for the application of these new compounds in corrosion protection

1. Introduction

Carbon steel has found wide application in various fields including automotive, ship and space rocket industries **[1]**. Unfortunately, one of the main problems associated with the use of carbon steel is its low corrosion resistance under aggressive environments. One of the methods for protecting metals from corrosion consists of introduction of inhibitors into the environment, which even at low concentration can significantly reduce the rate of corrosion **[2]**.

Organic molecules with specific functional groups have been used as corrosion inhibitors because of their effectiveness at wide range of temperatures, compatibility with protected materials, good solubility and relatively low toxicity**[3]**. The mechanism of action of organic corrosion inhibitors is typically based on the adsorption on the surface to form protective film. The adsorption process is influenced by the chemical structure of organic inhibitors, nature and surface charge, the distribution of charge within the molecule and medium composition **[2,4,5]**. During the last few years interest around the use of surfactants as corrosion inhibitors has significantly increased **[6–9]**. However, the huge consumption of surfactants, exceeding ten million tons on a global scale, with forecasts reaching 25 million tons in 2020, poses a serious threat to the natural environment. Therefore, intensive research is being conducted to obtain new, more effective surfactants, which would significantly reduce the number of surfactants used so far, and their operation would be in line with the principles of sustainable development.

Gemini surfactants are a class of surfactants consisting of two monomers of quaternary ammonium salts connected by a spacer **[10,11]**. Recent studies have focused on the study of such surfactants which, compared to the monomeric surfactants used so far, are better for the environment, less toxic, more thermally stable and have more favorable surface properties (e.g. surface tension) and antimicrobial activity**[12]**

In this work, we describe the synthesis and characterization of two novel gemini surfactants with the aim of correlating structural differences between them with their ability to inhibit corrosion in carbon steel under neutral conditions. The corrosion inhibition studies were carried out by electrochemical impedance spectroscopy (EIS), linear polarization resistance (LPR) and potentiodynamic polarization, and compared with the well-known organic corrosion inhibitor 1*H*-benzotriazole (BTA) [13,14]. The results obtained were then used to estimate surface adsorption parameters and compared with findings from DFT calculations.

2. Materials and methods

2.1. Chemicals

Bis[2-(*N*,*N*-dimethylamino)ethyl] ether (97%) was supplied by SigmaAldrich. Chloroesters were obtained from alcohols: 1 – octanol (99%, SigmaAldrich) and 1 – decanol (98%, SigmaAldrich) with appropriate amount of chloroacetic acid (99%, SigmaAldrich) under acidic conditions. Diethyl ether were purchased from AlChem. All chemicals were used without further purification.

2.2. Synthesis of cationic surfactants

Two novel surfactants were prepared by reaction of different chloroesters with appropriate amount of bis[2-(*N*,*N*-dimethylamino)ethyl] ether with the molar ratio 2:1 (**Figure 1**.).

The reactants were left under room temperature for 10 h without solvent. The products were crystallized from diethyl ether with addition of acetonitrile and then dried over P_4O_{10}.

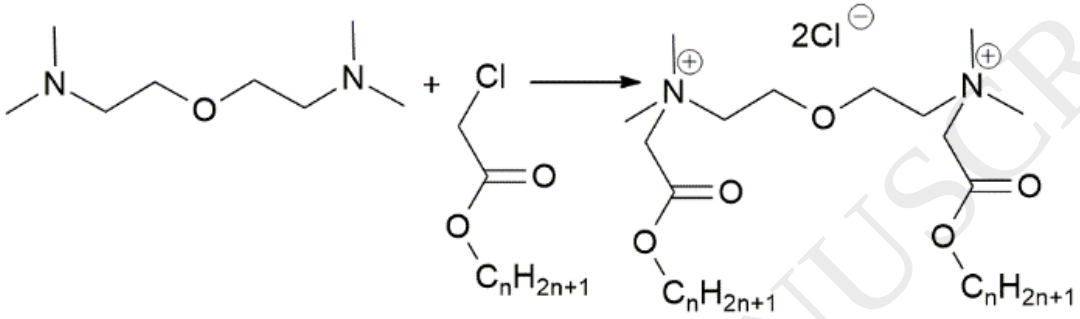

Figure 1. Synthesis of two new gemini surfactants.

2.3. Characterization methods

2.3.1. Spectroscopic and spectrometry characterization of gemini surfactants

The Nuclear Magnetic Resonance (NMR) spectra were measured with a Varian Mercury 300 MHz Spectrometer (Oxford, UK). The ^{13}C and ^{1}H chemical shifts were measured using $CDCl_3$ as a solvent with internal standard of TMS (tetramethylsilane).

2.3.2. Conductivity Measurement

Conductivity measurements were carried out using a (CO 300, VWR, Poland) Conductivity Meter with a 2-pole measuring cell (Ø 12 mm, stainless steel). The instrument was calibrated using a standard (147 µS/cm in 25 °C). Double distilled water was used in all the experimental work, and its specific conductivity value was around $1–2x10^{-6}$ S/cm.

2.3.3. Carbon steel

Corrosion tests were done with DC01 mild steel sample, with a chemical composition of C% 0.12, Mn% 0.6, P% max 0.045, S% 0.045 and balance in Fe. Each specimen surface was polished with emery paper from 600 up to 1000 grit.

2.3.4. Electrolytes

The electrolyte 50 mM NaCl was prepared by dissolving appropriate amount of NaCl (Sigma Aldrich) in distilled water. Solutions with different concentrations of inhibitors were prepared from the stock solution of 50 mM NaCl.

2.3.5. Electrochemical measurements

Electrochemical tests were carried out using a conventional three electrode cell with a platinum counter electrode, a saturated calomel electrode (SCE) as a reference electrode and a working electrode of mild steel DC01 plate at room temperature. The cell was placed in the Faraday cage to avoid the interference of external magnetic field.

Electrochemical impedance spectroscopy (EIS) measurements were carried out using a potentiostat (Gamry FAS2 Femtostat with a PCI4 Controller). Impedance spectra were obtained over a frequency range of 100 kHz to 10 mHz with a 10 mV sine wave as the excitation signal at open circuit potential. Linear polarization resistance measurements (LPR) were obtained by changing the potential from −20 to +20 mV versus OCP. Separate anodic and cathodic polarization curves were obtained by scanning the electrode potential from (cathodic) OCP to −300 mV vs the OCP and (anodic) OCP to +300 mV vs OCP after 24 immersion in 50Mm NaCl with different concentraions of inhibitors, respectively. EIS data was fitted with equivalent circuits using Gamry Echem Analyst (Version 6.25). The equivalent circuits used were based on RC circuits, using constant phase elements instead of pure capacitances. The goodness of fittings was evaluated by χ^2 (lower than $5x10^{-4}$).

2.3.6. Quantum calculations

The structures were optimized and calculated with DFT at B3LYP/6-31 G (d,p) level of the theory using GAUSSIAN 09' program [15–18]. The parameters of the investigated gemini surfactants were calculated, namely: energy of the molecule (E), energy of the highest occupied molecular orbital (E_{HOMO}), energy of the lowest unoccupied molecular orbital (E_{LUMO}), energy gap (ΔE), chemical hardness (η), softness (σ), ionization potential (I_P), electron affinity (E_A), electronegativity (χ), the fraction of electron transferred (ΔN) and dipole moment (μ) [19–24].

3. Results and discussion

3.1. Synthesis and spectroscopic characterization of gemini surfactants

The chemical structure of the synthesized compounds was characterized by ^1H NMR and ^{13}C NMR and is described below (see supplementary materials).

N2OE8 3-oxa-1,5-pentamethylene–bis(*N*-octyl-2-chloroacteate-*N*,*N* -dimethylammonium chloride)

^{1}H NMR (400 MHz, $CDCl_3$): δ/ppm 0.88 (t, 6H), 1.20-1.33 (m, 24H), 1.65 (t, 4H), 2.08 – 2.21 (m, 4H), 3.69 (s, 12H), 4.16 (t, 4H), 4.23-4.36 (m, 4H), 4.83 – 4.97 (m, 4H).

^{13}C NMR (75 MHz, $CDCl_3$) δ 165.04, 66.66, 64.61, 64.20, 62.05, 52.45, 31.84, 29.50, 29.44, 29.25, 29.16, 28.25, 25.61, 22.63, 14.06.

N2OE10 3-oxa-1,5-pentamethylene–bis(*N*-decyl-2-chloroacteate-*N,N* -dimethylammonium chloride)

^{1}H NMR (400 MHz, $CDCl_3$): δ/ppm 0.88 (t, 6H), 1.17-1.37 (m, 28H), 1.67 (t, 4H), 2.57-2.71 (m, 4H), 3.69 (s, 12H), 4.16 (t, 4H), 4.28-4.36 (m, 4H), 4.92 – 5.00 (m, 4H).

^{13}C NMR (75 MHz, $CDCl_3$) δ/ppm 165.04, 66.61, 64.61, 64.11, 62.03, 52.41, 31.86, 29.61, 29.58, 29.47, 29.31, 29.19, 28.26, 25.61, 22.64, 14.07.

3.2. CMC determination

The CMC of gemini surfactants depends on many factors such as alkyl chain length, number of quaternary ammonium atom, counterion, functionalization of spacer and hydrophobic chain [3,25–27]. In the present study, the influence of alkyl chain length on CMC point was the variable investigated. The CMC point was determined using a conductometric titration [25,28]. The plots of specific conductivity vs. concentration of the surfactant are presented in **Figure 2**. The CMC value was determined from the intersection of two slopes: pre and after micellization of surfactants [29,30]. It can be observed that an increase in alkyl chain length significantly decrease CMC value from 8.5mM to 1.7mM [26,31].

Parameters related to micelles formation obtained from conductivity measurements are presented in **Table 1**.

Counterion binding parameter (β) was calculated indirectly from degree of counter ion dissociation (α). α was calculated from plots of specific conductivity versus concentration (**Figure 2**.). Pre-

micellar slope (S_1) and post micellar slope (S_2) were used for the evaluation of the values as: $\alpha = S_2/S_1$. And then translated as: $\beta = 1 - \alpha$ [30].

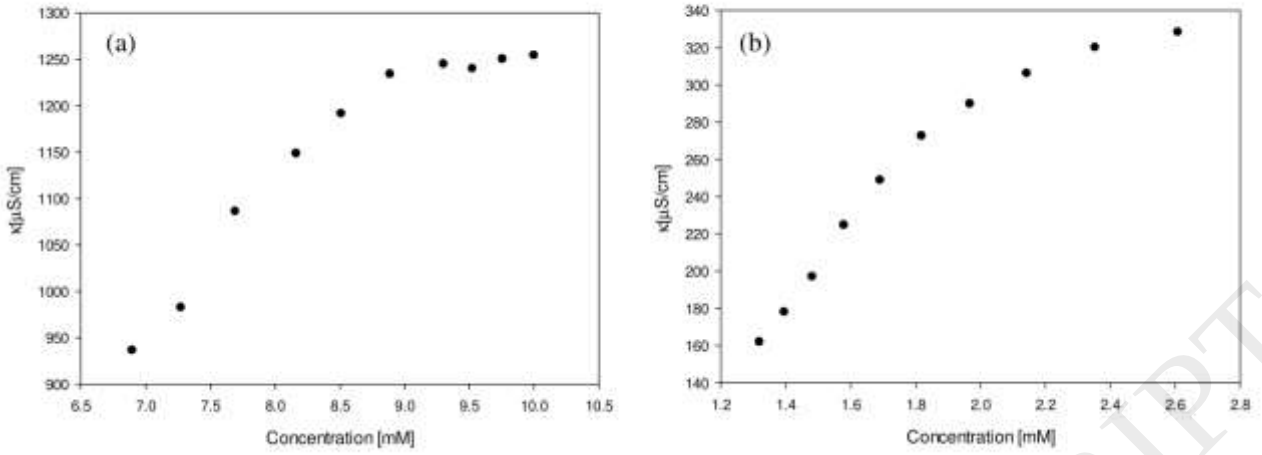

Figure 2. Plot of specific conductivity (κ) versus concentration of N2OE8 (a) and N2OE10(b) in water solution at 25 °C and pressure 0.1 MPa.

The ratio of the slopes of the linear regions above and below the CMC provides an estimation of the counterion binding parameter, β (**Figure 2**.). The standard Gibbs energy of micellisation ($\Delta G°_{mic}$) gives information as to whether micelles formation is spontaneous and can be calculated using the following expression [32]:

$$\Delta G°_{mic} = RT\left(\frac{1}{2}+\beta\right)\ln CMC - \left(\frac{RT}{2}\right)\ln 2 \qquad (1)$$

where β is the fraction of charges of micellised univalent surfactant ions neutralised by micelle–bound univalent counterions, the CMC is expressed in mol/dm^3, T is the temperature in Kelvin (K) and R is the gas constant.

Table 1. Critical micelle concentration (CMC), counterion binding parameter (β) and Gibbs free energy of micellization (ΔG°mic) of gemini surfactants obtained from conductivity measurements.

	CMC [mM]	**β**	**$\Delta G°_{mic}$ [kJ/mol]**
N2OE8	8.50±0.1	0.10±0.01	-7.95
N2OE10	1.72±0.08	0.29±0.04	-13.34

3.3. Polarization measurements

Table 2 presents parameters obtained from Tafel extrapolation of the polarization curves for different concentrations of gemini surfactants, while **Figure 3** depicts the cathodic and anodic curves for the most efficient concentrations. The addition of corrosion inhibitors in 50mM NaCl solution shifts the potential towards more noble values with respect to the reference. This is due to the adsorption of inhibitor molecules on the surface of mil steel and is further evidence that dimeric quaternary ammonium salts act as mixed inhibitors: they reduce anodic metal dissolution and retard the cathodic reactions as well [33].

The corrosion current density (i_{corr}) and inhibition efficiency (IE) were calculated as described below. The value of corrosion current density was determined indirectly by measuring the polarization resistance (R_P) and then using the Stern – Geary equation [34]:

$$i_{corr} = \frac{\beta_a \beta_c}{2.303(\beta_a + \beta_c)R_P} \quad (4)$$

where β_a, β_c are the slope coefficients of the anodic and cathodic Tafel lines [mV dec^{-1}], respectively, and R_P is the polarization resistance obtained from LPR measurements [Ωcm^2]. Then, the corrosion current density obtained can be used to estimate the corrosion inhibition efficiency using the following equation [35–37]:

$$IE\ (\%) = \frac{i_{0\ corr} - i_{corr}}{i_{0\ corr}}\ x\ 100\% \quad (5)$$

where $i_{0\ corr}$ and i_{corr} are the corrosion current density without and with surfactants inhibitors in solution, respectively.

The results presented in Table 2 show that E_{corr} values are displaced towards the anodic direction in the presence of surfactants, as qualitatively described above. However, both anodic and cathodic Tafel slopes change in the presence of these compounds, suggesting a mixed character of these inhibitors.

Table 2. Electrochemical parameters obtained from polarization curves after 24 h immersion with and without inhibitors in 50mM NaCl medium at room temperature.

	Concentration of surfactant/mM	E_{corr}/mV	i_{corr} /mA cm^{-2}	β_a / mV dec^{-1}	β_c /mV dec^{-1}	Inhibition efficiency [%]
50mM NaCl		-712±5	17.4±0.7	63	127	-
N2OE8	0.085	-658±3	8.5±0.2	157	61	51
	0.85	-656±5	7.3±0.2	103	54	58
	8.5	**-614±8**	**3.6±0.1**	**66**	**86**	**79**
	17	-655±4	8.4±0.1	88	66	51
N2OE10	0.017	-653±2	8.3±0.3	101	85	52
	0.17	-655±3	8.4±1.7	79	56	52
	1.7	**-687±4**	**6.6±0.4**	**87**	**122**	**62**
	3.4	-628±2	8.3±1.1	88	66	52

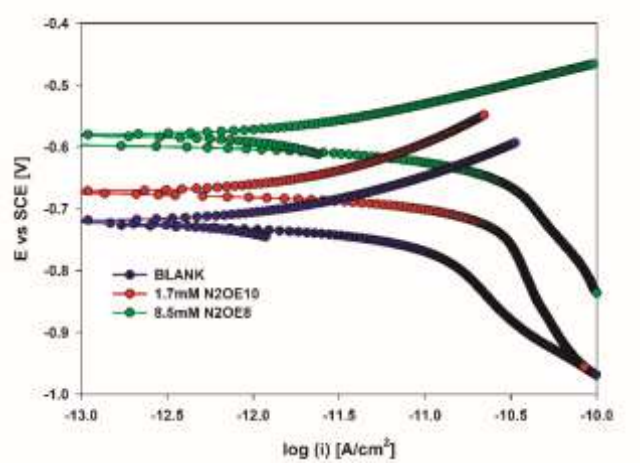

Figure 3. Polarization curves of carbon steel after 24h immersion in 50mM NaCl with and without inhibitor (for the most efficient concentrations) at room temperature.

The best corrosion inhibiting performance is achieved for concentrations of surfactants corresponding to the CMC values determined earlier. Under these conditions, the corrosion current density decreases more than 4 times in the presence of N2OE8, whereas in the case of N2OE10 the decrease in current density is 2-3 times corresponding to an inhibition efficiency of 79% and 62%, respectively.

A further increase in the concentration does not increase the inhibition effectiveness of the corrosion processes. This is due to less effective adsorption of molecules on the metal surface. At higher concentration, the inhibitor molecule begins to interact more with one another than with the metal surface [38].

3.4. Electrochemical impedance spectroscopy

Figure 4 depicts EIS spectra obtained for the surfactants N2OE8, N2OE10 after 24h and 1 month of immersion. Their performance is compared against the reference (bare) substrate and a 10 mM BTA solution. After 24 h of immersion in NaCl, the reference specimen shows the lowest impedance values among the systems studied. In this case, two overlapped time constants occurring around 10 Hz are detected and can be ascribed to deposits of corrosion products and ongoing corrosion processes at the surface. In the presence of BTA, the low frequency impedance magnitude values are larger than the reference. In this case, the detected time constant is found at ~1 Hz. Although not well visible, a second time constant at higher frequencies, overlapped with the former, seems to be present around 10 Hz and may be due to the adsorption layer of BTA together with corrosion products. The best performing systems are those in the presence of the gemini surfactants, with $|Z|_{0.01Hz}$ for N2OE8 and N2OE10 more than twice larger than |Z| for the reference system. In these cases, one time constant is detected at ca. ~1 Hz, related to the corrosion processes occurring at the metal surface, superposed with another intermediate time constant (10-100Hz) that may be related to deposits of surfactant.

With increase of immersion time up to 1 month, the best performing systems are still the gemini surfactants, followed by BTA. Nevertheless, the $|Z|_{0.01Hz}$ follow opposite trends: for the N2OE10 the impedance magnitude increased with the immersion time, while for N2OE8 there was a decrease in the impedance magnitude.

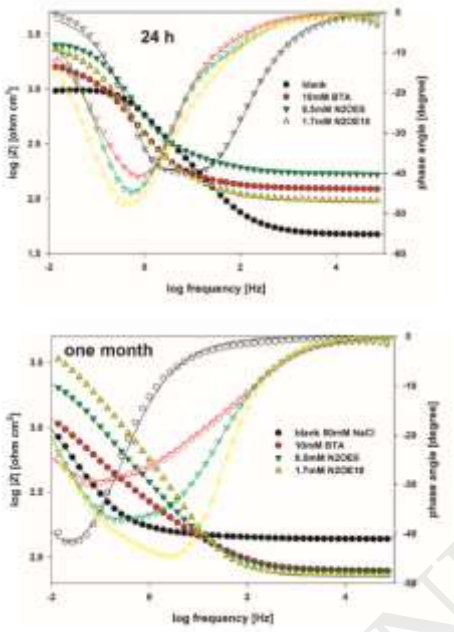

Figure 4. EIS results of the DC01 in 50mM NaCl with corrosion inhibitors: BTA, N2OE8, N2OE10.

Furthermore, analyzing the phase angle plot, BTA, N2OE8 and N2OE10 show well-defined two time constant processes, one around 10 Hz and another around 0.1 Hz. Again, the first can be due to buildup of adsorbing layer on the surface, whereas the latter can be ascribed to the corrosion processes occurring at the metal interface.

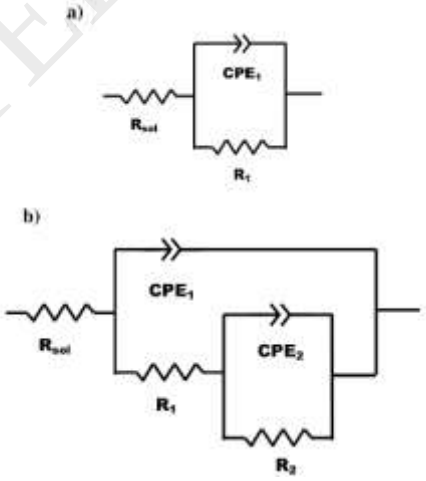

Figure 5. Electrical equivalent circuits used to fit EIS presented in Figure 4.

Table 3: Fitted parameters of the low frequency time-constant present in EIS spectra depicted in Figure 3, using the EC circuits presented in Figure 4.

	Blank	BTA	N2OE8	N2OE10

1 day	**C/Fcm^{-2}**	2.00x10^{-4}	1.18x10^{-4}	2.30x10^{-4}	2.98x10^{-4}
	R/Ωcm^2	4.62x10^2	1.48x10^3	2.97x10^3	2.36x10^3
1 month	**C/Fcm^{-2}**	2.19x10^{-2}	1.86x10^{-2}	4.82x10^{-4}	1.33x10^{-3}
	R/Ωcm^2	2.62x10^3	7.43x10^3	4.39x10^3	4.16x10^3

Effective capacitance C_{eff} was estimated using the equation $C_{eff} = Q^{1/n}R^{(1-n)/n}$ [39,40].

All the experimental data was fitted using equivalent circuits described in **Figure 5**. Except for the reference system after one month (**Figure 5a**), all the others were fitted using a two-time constant RCPE circuit (**Figure 5b**). However, the assignment of time constants is not straightforward. Surface heterogeneity/roughness or even mass-controlled processes seem to already play some influence on the results of all the systems after 24h, since the effective capacitance values are in the order of 10^{-4} F cm^{-2}, whereas the capacitance associated with the double layer is typically around 10^{-5} F cm^{-2} [41,42]

In the case of both reference and BTA systems, the effective capacitance estimated from CPE values after one month are two orders of magnitude larger than the capacitance estimated from CPE after 24h of immersion (10^{-2} F cm^{-2} *vs.* 10^{-4} F cm^{-2}, respectively). This, together with a *n* value for the CPE around 0.5 and phase angles around 45º points towards diffusion-controlled processes.

However, this trend was not found for the gemini surfactant systems (Table 3). In fact, the estimated effective capacitance increased in less extent for these systems (most notably for N2OE8), which may be related to the capacity of the adsorbed layer in controlling the degradation of the substrate.

3.5. Adsorption isotherm

The analysis of adsorption isotherms can provide information on how the surfactant molecules interact with the metal surface. The degree of surface coverage (Θ) for different concentration of inhibitors has been evaluated by using following equation [8,43,44]:

$$\theta = \frac{IE\%}{100} \quad (7)$$

where the IE% is the inhibition efficiency obtained from LPR.

Assuming that the Langmuir adsorption isotherm applies, the graphs of C/θ vs. C were presented in **Figure 6** allows the estimation of the constant of adsorption K_{ads} [45].

The change in the Gibbs free energy (ΔG_{ads}) was determined with the following equation [46–48]

$$\Delta G_{ads} = - RT\ln (55.5K_{ads}) \quad (8)$$

where R is the gas constant, T is the temperature, the value 55.5 is the molar concentration of water, and K_{ads} equilibrium adsorption constant [49].

The ΔG_{ads} values provide information about the nature of the process. Negative values indicate that the process is spontaneous [50]. A negative value of ΔG demonstrates that the adsorption of surfactant on the steel surface is a spontaneous process and shows a strong interaction between surfactant molecules and steel surface.

Table 4. Data obtained from Langmuir isotherm model for N2OE8 and N2OE10 for mild steel in 50mM NaCl

	R^2	K_{ads} [dm^3/mol]	ΔG_{ads} [kJ/mol]
N2OE8	0.99	1.92±0.51	-11.46±0.72
N2OE10	0.96	8.01±1.03	-15.08±0.34

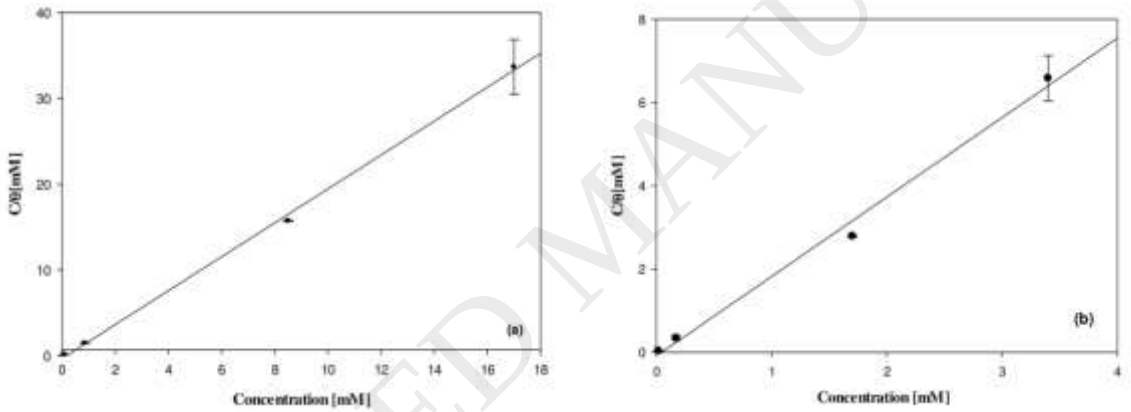

Figure 6. Langmuir isotherm adsorption model of (a) N2OE8 and (b) N2OE10 for mild steel in 50mM NaCl.

3.6. Quantum calculations

The optimized structures of investigated compounds calculated by DFT at B3LYP/6-31 G (d,p) are presented in **Table 5**.

Table 5. Optimised structure, HOMO and LUMO density presented based on DFT calculations calculated by B3LYP/6-31G(d).

	N2OE8	*N2OE10*
Optimized structure	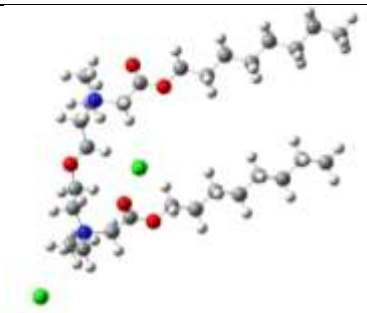	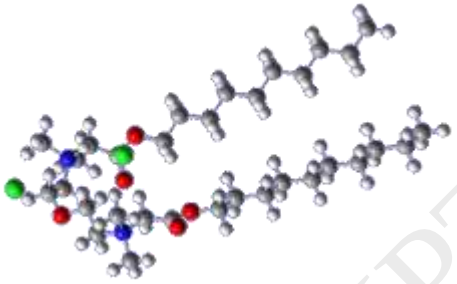
HOMO	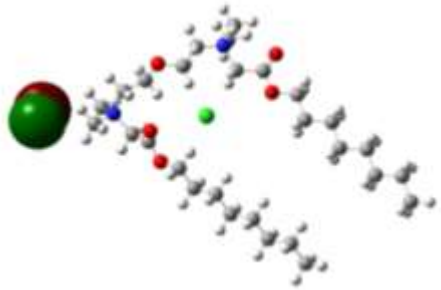	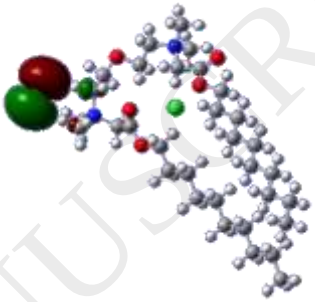
LUMO	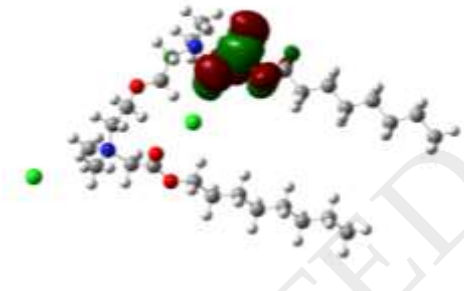	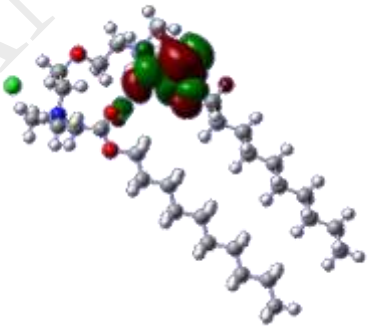

DFT calculations provide information about theoretical ability to inhibit corrosion based on: total energy of the molecule (E), energy of the highest occupied orbital (E_{HOMO}), energy of the lowest free orbital (E_{LUMO}), energy gap (ΔE), hardness (η), softness (σ), ionization potential (I_P), electron affinity (E_A), electronegativity (χ), electron transfer fraction (ΔN) and dipole moment (μ) and then associate it with the corrosion inhibiting ability [51–56]. Parameters obtained from quantum calculations were summarised in **Table 6**.

Table 6. Theoretical parameters for investigated compounds.

Quantum chemical parameters	N2OE8	N2OE10
E [keV]	-68.24	-75.51
μ [Debye]	29.789	16.196
E_{HOMO} [eV]	-0.11698	-0.16685
E_{LUMO} [eV]	-0.06198	-0.04683
ΔE [eV][1]	0.055	0.120
σ [eV^{-1}][2]	36.36	16.66
η [eV][3]	0.0275	0.06001
I_p [eV][4]	0.11698	0.16685
E_A [eV][5]	0.06198	0.04683
χ [eV][6]	0.14797	0.190265
ΔN [eV]	-124.582	-56.7383

[1]$\Delta E = E_{LUMO} - E_{HOMO,}$, [2]$\sigma = 1/\eta$, [3]$\eta = - ½ (E_{HOMO} – E_{LUMO})$, [4]$I_p = -E_{HOMO,}$ [5]$E_A = -E_{LUMO,}$ [6]$\chi = (IP + EA)/2$

The structure of each compound was optimised by functional density B3LYP and base 6-31G (d,p). N2OE8 and N2OE10 reached energy lower than zero, it indicates that structures are thermodynamically stable [57]. E_{HOMO} is associated with the ability of the inhibitor molecule to donate free electron pairs. E_{LUMO} is related to the ability to accept electrons from the metal. Both surfactants studied in this work show negative E_{HOMO} values, meaning that the corrosion inhibition process should be based on physical adsorption [51].

If the energy gap is relatively low it means that the molecule is much more reactive to adsorb into the metal surface. In principle N2OE8 should be a more efficient inhibitor than N2OE10, because the energy gap is much smaller [58].

The dipole moment (μ) is a factor that can also provide information about interaction between positively charged inhibitor molecule and negatively charged metal surface. If the value is higher, the stronger interactions between surface and molecules can be observed. The higher value possesses N2OE8, which indicate stronger adsorption [19,22].

Chemical hardness (η) and softness (σ) provide information about the resistance of a molecule to transfer charge and about the capacity of a molecule to receive electrons. A higher σ value suggests greater tendency to donate electrons to the metal [24]. This parameter is significantly higher for N2OE8 when compared to N2OE10, which confirm the previous statements [20,54].

A high value of electronegativity (χ) suggest strong ability to attract electrons from the metal, which leads to greater interaction and possibly high corrosion protection. The value of electronegativity in case of investigated compounds are similar. The last parameter which can be

calculated is the fraction of electron transferred (ΔN) which is useful in their ability to help predict chemical behavior [6,59]:

$$\Delta N = \chi Fe - \chi inh / 2(\eta Fe - \eta inh) \quad (9)$$

where χFe equals 7eV and ηFe = 0. If ΔN > 0 the electrons are transferred from the molecule to the metal and if ΔN<0 from the metal to the molecule. For the tested gemini surfactants the values of the fraction of electron transferred are negative, indicating transfer from the metal to the molecules [19,52,60].

3.7. Discussion

The mechanism by which gemini surfactants can impart corrosion inhibition has been presented earlier [61] and is schematically shown below. The functional group in surfactant molecules is attracted to surfaces of metals and metal oxides. The attraction to surfaces is enhanced by the hydrophobic tail of the molecule that is attracted to other hydrophobic segments of adjacent surfactant molecules on surfaces. Thus, there is a driving force for surfactant adsorption on metal and metal oxide surfaces that orients the surfactant with the hydrophilic group at the solid interface and the hydrophobic hydrocarbon chain directed out into the solution, thereby creating a hydrophobic surface (**Figure 7**). This driving force causes surfactant molecules to aggregate on surfaces.

The main parameter which characterize a surfactant in aqueous solution is CMC (Critical Micelle Concentration) [29,31]. In low-concentration solutions, these compounds are present as single molecules. Increasing the concentration of surfactant leads to a gradual increase in its adsorption at the interface. When the surface of the interface is filled with molecules surfactant, then a further increase in the concentration of this compound increases its amount in the entire volume of the solution. Consistent increase in the amount of surfactant molecules leads to their organization into micelles.

The electrochemical measurements carried out showed that the presence of gemini surfactants leads to a reduction in the corrosion rate estimated from LPR, with the best results obtained for concentrations near the CMC and with the compound N2OE8 exhibiting better performance than N2OE10. In addition, EIS measurements carried out for short and long immersion times demonstrated the positive effect imparted by these compounds in the protection of mild steel substrate, better than the protective action rendered by well-known BTA molecules.

The adsorption of isotherm estimated from the inhibition efficiency is consistent with Langmuir isotherm, while the DFT calculations point towards N2OE8 as more appropriate molecule for adsorption than N2OE10, with the experimental electrochemical results supporting this

assumption and denoting that increase in the alkyl chain length results in lower corrosion protection.

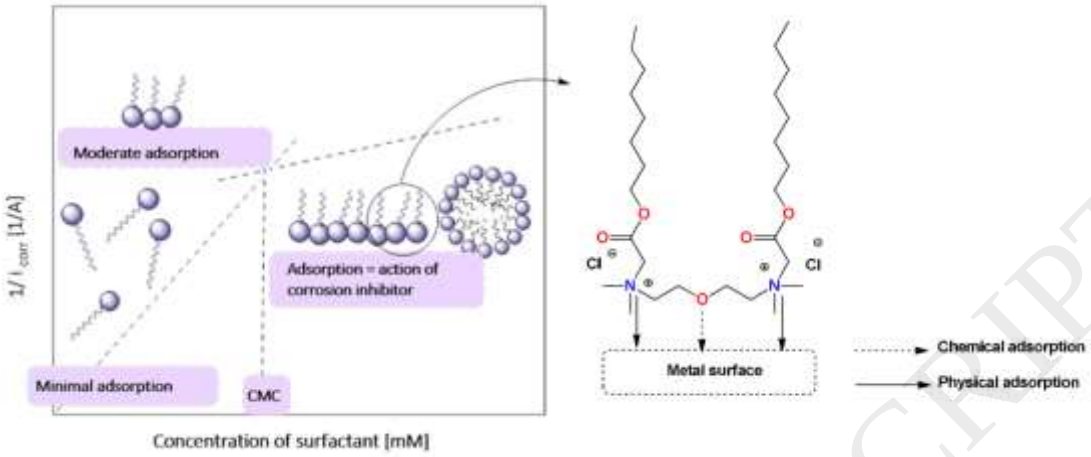

Figure 7. Correlation between CMC and adsorption in to the metal surface, mechanism of action gemini surfactant as corrosion inhibitor

4. Conclusions

Two new gemini surfactants were synthesized for the first time and their structure confirmed by NMR. Electrochemical studies performed for different concentrations showed that the highest corrosion inhibition efficiency is achieved at the CMC, which is consistent with the mechanism proposed for this type of compounds. Quite relevant is the higher corrosion protection achieved in the presence of both gemini surfactants when compared to commercially available corrosion inhibitor 1H-benzotriazole, even for long immersion times. The results obtained and the ranking of the gemini surfactants can be explained by differences in adsorption due to differences in the electronic properties of the molecules, as investigated by theoretical studies. Overall, these findings show that this class of molecules can play a role in corrosion protection of steel substrates used in different applications.

Conflicts of interest

There are no conflicts to declare

Acknowledgements

This work was supported by National Centre for Research and Development (Poland; TANGO1/266340/NCBR/2015).

This work was also developed within the scope of the project CICECO-Aveiro Institute of Materials, FCT Ref. UID/CTM/50011/2019, financed by national funds through the FCT/MCTES.

5. References

[1] A. Calik, A. Duzgun, O. Sahin, N. Ucar, Effect of Carbon Content on the Mechanical Properties of Medium Carbon Steels, Zeitschrift Für Naturforschung A. 65 (2010). doi:10.1515/zna-2010-0512.

[2] B.E. Brycki, I.H. Kowalczyk, A. Szulc, O. Kaczerewska, M. Pakiet, Organic Corrosion Inhibitors, in: M. Aliofkhazraei (Ed.), Corrosion Inhibitors, Principles and Recent Applications, InTech, 2018. doi:10.5772/intechopen.72943.

[3] B.E. Brycki, I.H. Kowalczyk, A. Szulc, O. Kaczerewska, M. Pakiet, Multifunctional Gemini Surfactants: Structure, Synthesis, Properties and Applications, in: R. Najjar (Ed.), Application and Characterization of Surfactants, InTech, 2017. doi:10.5772/intechopen.68755.

[4] M.P. Desimone, G. Grundmeier, G. Gordillo, S.N. Simison, Amphiphilic amido-amine as an effective corrosion inhibitor for mild steel exposed to CO2 saturated solution: Polarization, EIS and PM-IRRAS studies, Electrochimica Acta. 56 (2011) 2990–2998. doi:10.1016/j.electacta.2011.01.009.

[5] K. Xhanari, M. Finšgar, Organic corrosion inhibitors for aluminium and its alloys in acid solutions: a review, RSC Advances. 6 (2016) 62833–62857. doi:10.1039/C6RA11818F.

[6] O. Kaczerewska, R. Leiva-Garcia, R. Akid, B. Brycki, I. Kowalczyk, T. Pospieszny, Effectiveness of O -bridged cationic gemini surfactants as corrosion inhibitors for stainless steel in 3 M HCl: Experimental and theoretical studies, Journal of Molecular Liquids. 249 (2018) 1113–1124. doi:10.1016/j.molliq.2017.11.142.

[7] M. Pakiet, I.H. Kowalczyk, R. Leiva Garcia, R. Akid, B.E. Brycki, Influence of different counterions on gemini surfactants with polyamine platform as corrosion inhibitors for stainless steel AISI 304 in 3 M HCl, Journal of Molecular Liquids. 268 (2018) 824–831. doi:10.1016/j.molliq.2018.07.120.

[8] M.A. Hegazy, M. Abdallah, H. Ahmed, Novel cationic gemini surfactants as corrosion inhibitors for carbon steel pipelines, Corrosion Science. 52 (2010) 2897–2904. doi:10.1016/j.corsci.2010.04.034.

[9] F.A. Ansari, M.A. Quraishi, Inhibitive performance of gemini surfactants as corrosion inhibitors for mild steel in formic acid, Portugaliae Electrochimica Acta. 28 (2010) 321–335.

[10] F.M. Menger, C.A. Littau, Gemini-surfactants: synthesis and properties, Journal of the American Chemical Society. 113 (1991) 1451–1452. doi:10.1021/ja00004a077.

[11] R. Zana, Gemini (dimeric) surfactants, Current Opinion in Colloid & Interface Science. 1 (1996) 566–571. doi:10.1016/S1359-0294(96)80093-8.

[12] H. Kunieda, N. Masuda, K. Tsubone, Comparison between Phase Behavior of Anionic Dimeric (Gemini-Type) and Monomeric Surfactants in Water and Water−Oil, Langmuir. 16 (2000) 6438–6444. doi:10.1021/la0001068.

[13] M.G. Hosseini, M.R. Arshadi, T. Shahrabi, M. Ghorbani, Synergistic influence of benzoate ions on inhbition of corrosion of mild steel in 0.5M sulphuric acid by benzotriazole, IJE Transactions B: Applications. 16 (n.d.) 255–264.

[14] G.K. Gomma, Corrosion inhibition of steel by benzotriazole in sulphuric acid, Materials Chemistry and Physics. 55 (1998) 235–240. doi:10.1016/S0254-0584(98)00043-1.

[15] J.J.P. Stewart, Optimization of parameters for semiempirical methods V: Modification of NDDO approximations and application to 70 elements, Journal of Molecular Modeling. 13 (2007) 1173–1213. doi:10.1007/s00894-007-0233-4.

[16] J.J.P. Stewart, Optimization of parameters for semiempirical methods I. Method, Journal of Computational Chemistry. 10 (1989) 209–220. doi:10.1002/jcc.540100208.
[17] J.J.P. Stewart, Optimization of parameters for semiempirical methods. III Extension of PM3 to Be, Mg, Zn, Ga, Ge, As, Se, Cd, In, Sn, Sb, Te, Hg, Tl, Pb, and Bi, Journal of Computational Chemistry. 12 (1991) 320–341. doi:10.1002/jcc.540120306.
[18] M. J. Frisch, G. W. Trucks, H. B. Schlegel, G. E. Scuseria, M. A., Robb, J. R. Cheeseman, G. Scalmani, V. Barone, B. Mennucci, G. A. Petersson, H. Nakatsuji, M. Caricato, X. Li, H. P. Hratchian, A. F. Izmaylov, J. Blonio, G. Zheng, J. L. Sonnenberg, M. Hada, M., Ehara, K. Toyota, R. Fakuda, J. Hasegawa, M. Ishida, T. Nakajima, Y. Honda, O. Kitao, H. Nakai, T. Verven, J. A. Montgomery, J. E., Peralta, F. Ogliaro, M. Bearpark, J. J. Heyd, E. Brothers, K. N., Kudin, V. N. Staroverov, T. Keith, R. Kobayashi, J. Normad, K., Raghavachari, A. Rendell, J. C. Burant, S. S. Iyengar, J. Tomasi, M., Cossi, N. Rega, J. M. Millam, M. Klene, J. E. Knox, J. B. Cross, V., Bakken, C. Adamo, J. Jaramillo, R. Gomperts, R. E. Stratmann, O., Yazyev, A. J. Austin, R. Cammi, C. Pomelli, J. W. Ochterski, R. L., Martin, K. Morokuma, V. G. Zakrzewski, G. A. Voth, P. Salvador, J. J. Dannenberg, S. Dapprich, A. D. Daniels, O. Farkas, J. B., Forseman, J. V. Ortiz, J. Cislowski, D. J. Fox, G, GAUSSIAN 09 Revision B.01, GAUSSIAN 09 Revision B.01. (2010).
[19] D.K. Verma, Density Functional Theory (DFT) as a Powerful Tool for Designing Corrosion Inhibitors in Aqueous Phase, in: A. Ali (Ed.), Advanced Engineering Testing, InTech, 2018. doi:10.5772/intechopen.78333.
[20] A. Singh, K. R. Ansari, M. A. Quraishi, Y. Lin, Investigation of Corrosion Inhibitors Adsorption on Metals Using Density Functional Theory and Molecular Dynamics Simulation, in: Corrosion Inhibitors [Working Title], IntechOpen, 2019. doi:10.5772/intechopen.84126.
[21] P. Udhayakala, Density functional theory calculations on corrosion inhibitory action of five azlactones on mild steel, (2014) 11.
[22] V.S. Sastri, J.R. Perumareddi, Molecular Orbital Theoretical Studies of Some Organic Corrosion Inhibitors, CORROSION. 53 (1997) 617–622. doi:10.5006/1.3290294.
[23] S.R. Gupta, P. Mourya, M.M. Singh, V.P. Singh, Structural, theoretical and corrosion inhibition studies on some transition metal complexes derived from heterocyclic system, Journal of Molecular Structure. 1137 (2017) 240–252. doi:10.1016/j.molstruc.2017.02.047.
[24] G. Gece, The use of quantum chemical methods in corrosion inhibitor studies, Corrosion Science. 50 (2008) 2981–2992. doi:10.1016/j.corsci.2008.08.043.
[25] H. Zhu, Z. Hu, D. Liang, J. Wang, D. Cao, Aggregation of diester-bonded cationic gemini surfactants in the presence of ethylene glycol: An electrical conductivity study, Journal of Molecular Liquids. 216 (2016) 565–570. doi:10.1016/j.molliq.2016.01.067.
[26] M.T. Garcia, O. Kaczerewska, I. Ribosa, B. Brycki, P. Materna, M. Drgas, Hydrophilicity and flexibility of the spacer as critical parameters on the aggregation behavior of long alkyl chain cationic gemini surfactants in aqueous solution, Journal of Molecular Liquids. 230 (2017) 453–460. doi:10.1016/j.molliq.2017.01.053.
[27] M.I. Nessim, M.M. Osman, D.A. Ismail, Surface-active properties of new cationic gemini surfactants with cyclic spacer, Journal of Dispersion Science and Technology. 39 (2018) 1047–1055. doi:10.1080/01932691.2017.1381916.
[28] A. Pinazo, X. Wen, L. Pérez, M.-R. Infante, E.I. Franses, Aggregation Behavior in Water of Monomeric and Gemini Cationic Surfactants Derived from Arginine, Langmuir. 15 (1999) 3134–3142. doi:10.1021/la981295l.
[29] V. Singh, R. Tyagi, Unique Micellization and CMC Aspects of Gemini Surfactant: An Overview, Journal of Dispersion Science and Technology. 35 (2014) 1774–1792. doi:10.1080/01932691.2013.856317.
[30] Kabir-ud-Din, P.A. Koya, Z.A. Khan, Conductometric studies of micellization of gemini surfactant pentamethylene-1,5-bis(tetradecyldimethylammonium bromide) in water and water–organic solvent

mixed media, Journal of Colloid and Interface Science. 342 (2010) 340–347. doi:10.1016/j.jcis.2009.10.056.
[31] R. Zana, Critical Micellization Concentration of Surfactants in Aqueous Solution and Free Energy of Micellization, Langmuir. 12 (1996) 1208–1211. doi:10.1021/la950691q.
[32] R. Zana, Critical micellization concentration of surfactants in aqueous solution and free energy of micellization, Langmuir. 12 (1996) 1208–1211.
[33] F. Mansfeld, Tafel slopes and corrosion rates obtained in the pre-Tafel region of polarization curves, Corrosion Science. 47 (2005) 3178–3186. doi:10.1016/j.corsci.2005.04.012.
[34] E. Machnikova, K.H. Whitmire, N. Hackerman, Corrosion inhibition of carbon steel in hydrochloric acid by furan derivatives, Electrochimica Acta. 53 (2008) 6024–6032. doi:10.1016/j.electacta.2008.03.021.
[35] P.O. Ameh, N.O. Eddy, Theoretical and experimental studies on the corrosion inhibition potentials of 3-nitrobenzoic acid for mild steel in 0.1 M H2SO4, Cogent Chemistry. 2 (2016). doi:10.1080/23312009.2016.1253904.
[36] S.M. Shaban, A. Saied, S.M. Tawfik, A. Abd-Elaal, I. Aiad, Corrosion inhibition and Biocidal effect of some cationic surfactants based on Schiff base, Journal of Industrial and Engineering Chemistry. 19 (2013) 2004–2009. doi:10.1016/j.jiec.2013.03.013.
[37] M.O. Agafonkina, N.P. Andreeva, Yu.I. Kuznetsov, S.F. Timashev, Substituted benzotriazoles as inhibitors of copper corrosion in borate buffer solutions, Russian Journal of Physical Chemistry A. 91 (2017) 1414–1421. doi:10.1134/S0036024417080027.
[38] Y. Zhu, M.L. Free, R. Woollam, W. Durnie, A review of surfactants as corrosion inhibitors and associated modeling, Progress in Materials Science. 90 (2017) 159–223. doi:10.1016/j.pmatsci.2017.07.006.
[39] B. Hirschorn, M.E. Orazem, B. Tribollet, V. Vivier, I. Frateur, M. Musiani, Determination of effective capacitance and film thickness from constant-phase-element parameters, Electrochimica Acta. 55 (2010) 6218–6227. doi:10.1016/j.electacta.2009.10.065.
[40] G.J. Brug, A.L.G. Van Den Eeden, M. Sluyters-Rehbach, J.H. Sluyters, The analysis of electrode impedances complicated by the presence of a constant phase element, J. Electroanal. Chem. (1984) 275–295.
[41] E. McCafferty, N. Hackerman, Double Layer Capacitance of Iron and Corrosion Inhibition with Polymethylene Diamines, Journal of The Electrochemical Society. 119 (1972) 146. doi:10.1149/1.2404150.
[42] S. Amand, M. Musiani, M.E. Orazem, N. Pébère, B. Tribollet, V. Vivier, Constant-phase-element behavior caused by inhomogeneous water uptake in anti-corrosion coatings, Electrochimica Acta. 87 (2013) 693–700. doi:10.1016/j.electacta.2012.09.061.
[43] F. Kellou-Kerkouche, A. Benchettara, S.-E. Amara, Anionic Surfactant as a Corrosion Inhibitor for Synthesized Ferrous Alloy in Acidic Solution, Journal of Materials. 2013 (2013) 1–11. doi:10.1155/2013/903712.
[44] S. Stolnik, B. Daudali, A. Arien, J. Whetstone, C.R. Heald, M.C. Garnett, S.S. Davis, L. Illum, The effect of surface coverage and conformation of poly (ethylene oxide)(PEO) chains of poloxamer 407 on the biological fate of model colloidal drug carriers, Biochimica et Biophysica Acta (BBA)-Biomembranes. 1514 (2001) 261–279.
[45] R.J. Chin, K. Nobe, Electrochemical characteristics of iron in H 2 SO 4 containing benzotriazole, Journal of the Electrochemical Society. 118 (1971) 545–548.
[46] S. Manimegalai, P. Manjula, Thermodynamic and Adsorption studies for corrosion Inhibition of Mild steel in Aqueous Media by Sargasam swartzii (Brown algae), Journal of Material and Environmental Science. 6 (2015) 1629–1637.
[47] M. Abdallah, H.M. Eltass, M.A. Hegazy, H. Ahmed, Adsorption and inhibition effect of novel cationic surfactant for pipelines carbon steel in acidic solution, Protection of Metals and Physical Chemistry of Surfaces. 52 (2016) 721–730. doi:10.1134/S207020511604002X.

[48] I. Danaee, O. Ghasemi, G.R. Rashed, M. Rashvand Avei, M.H. Maddahy, Effect of hydroxyl group position on adsorption behavior and corrosion inhibition of hydroxybenzaldehyde Schiff bases: Electrochemical and quantum calculations, Journal of Molecular Structure. 1035 (2013) 247–259. doi:10.1016/j.molstruc.2012.11.013.
[49] Chem. Dep., Faculty of Applied Sciences, Umm Al-Qura University, Makkah, Saudi Arabia., M. Abdallah, Corrosion Inhibition of Stainless Steel Type 316 L in 1.0 M HCl Solution Using 1,3-Thiazolidin-5-one Derivatives, International Journal of Electrochemical Science. (2017) 4543–4562. doi:10.20964/2017.05.35.
[50] R. Karthikaiselvi, S. Subhashini, Study of adsorption properties and inhibition of mild steel corrosion in hydrochloric acid media by water soluble composite poly (vinyl alcohol-omethoxy aniline), Journal of the Association of Arab Universities for Basic and Applied Sciences. 16 (2014) 74–82. doi:10.1016/j.jaubas.2013.06.002.
[51] G. Gece, The use of quantum chemical methods in corrosion inhibitor studies, Corrosion Science. 50 (2008) 2981–2992. doi:10.1016/j.corsci.2008.08.043.
[52] G. Gao, C. Liang, Electrochemical and DFT studies of β-amino-alcohols as corrosion inhibitors for brass, Electrochimica Acta. 52 (2007) 4554–4559. doi:10.1016/j.electacta.2006.12.058.
[53] K. Sayin, D. Karakaş, Quantum chemical studies on the some inorganic corrosion inhibitors, Corrosion Science. 77 (2013) 37–45. doi:10.1016/j.corsci.2013.07.023.
[54] O. Kaczerewska, R. Leiva- Garcia, R. Akid, B. Brycki, I. Kowalczyk, T. Pospieszny, Heteroatoms and π electrons as favorable factors for efficient corrosion protection, Materials and Corrosion. 70 (2019) 1099–1110. doi:10.1002/maco.201810570.
[55] E.A.M. Gad, E.M.S. Azzam, S.A. Halim, Theoretical approach for the performance of 4-mercapto-1-alkylpyridin-1-ium bromide as corrosion inhibitors using DFT, Egyptian Journal of Petroleum. 27 (2018) 695–699. doi:10.1016/j.ejpe.2017.10.005.
[56] E.E. Oguzie, Y. Li, S.G. Wang, F. Wang, Understanding corrosion inhibition mechanisms—experimental and theoretical approach, RSC Advances. 1 (2011) 866. doi:10.1039/c1ra00148e.
[57] F.E.-T. Heakal, A.E. Elkholy, Gemini surfactants as corrosion inhibitors for carbon steel, Journal of Molecular Liquids. 230 (2017) 395–407.
[58] I. Lukovits, E. Kálmán, F. Zucchi, Corrosion Inhibitors—Correlation between Electronic Structure and Efficiency, CORROSION. 57 (2001) 3–8. doi:10.5006/1.3290328.
[59] V.S. Sastri, J.R. Perumareddi, Molecular Orbital Theoretical Studies of Some Organic Corrosion Inhibitors, CORROSION. 53 (1997) 617–622. doi:10.5006/1.3290294.
[60] N.A. Wazzan, F.M. Mahgoub, DFT Calculations for Corrosion Inhibition of Ferrous Alloys by Pyrazolopyrimidine Derivatives, Open Journal of Physical Chemistry. 04 (2014) 6–14. doi:10.4236/ojpc.2014.41002.
[61] M. Lagren, F. Bentiss, Study of the mechanism and inhibiting e • ciency of 3,5-bis(4-methylthiophenyl)- 4H-1,2,4-triazole on mild steel corrosion in acidic media, Corrosion Science. (2002) 16.